JPET Fast Forward. Published on January 19, 2012 as DOI: 10.1124/jpet.111.190173

JPET # 190173

Role of CYP2A5 in the Bioactivation of the Lung Carcinogen 4-(Methylnitrosamino)-1-(3-Pyridyl)-1-Butanone in Mice

Xin Zhou, Jaime D'Agostino, Fang Xie, and Xinxin Ding

Laboratory of Molecular Toxicology, Wadsworth Center, New York State Department of Health, and School of Public Health, SUNY at Albany, Albany, NY 12201

JPET Fast Forward. Published on January 19, 2012 as DOI: 10.1124/jpet.111.190173
This article has not been copyedited and formatted. The final version may differ from this version.

JPET # 190173

RUNNING TITLE: *CYP2A5 and target tissue NNK bioactivation*

ADDRESS CORRESPONDENCE TO:

Dr. Xinxin Ding, Wadsworth Center, New York State Department of Health, Empire State Plaza, Box 509, Albany, NY 12201-0509

Tel. 518-486-2585; Fax: 518-473-8722; E-mail: xding@wadsworth.org

Number of Text Pages:	23	
Number of Tables:	3	
Number of Figures:	4 (plus one scheme)	
Number of References:	39	
Number of Words:	Abstract	249
	Introduction	711
	Discussion	1422
Supplemental material:	2 Figures, 1 Table	

ABBREVIATIONS: P450, cytochrome P450; LC, liquid chromatography; MS, mass spectrometry; HPB, 4-hydroxy-1-(3-pyridyl)-1-butanone; NNK-N-oxide, 4-(methylnitrosamino)-1-(3-pyridyl-N-oxide)-1-butanone; OPB, 4-oxo-4-(3-pyridyl)butanone; OPBA, 4-oxo-4-(3-pyridyl)butyric acid; NNK, 4-(methylnitrosamino)-1-(3-pyridyl)-1-butanone; NNAL, 4-(methylnitrosamino)-1-(3-pyridyl)-1-butanol; O^6-mG, O^6-methylguanine; 8-MOP, 8-methoxypsoralen; WT, wild-type; NADPH, reduced β-nicotinamide adenine dinucleotide phosphate; MIM-EPI, multiple ion monitoring-dependent enhanced product ion; MRM, multiple reaction monitoring.

SECTION ASSIGNMENT: Toxicology

JPET Fast Forward. Published on January 19, 2012 as DOI: 10.1124/jpet.111.190173
This article has not been copyedited and formatted. The final version may differ from this version.

ABSTRACT

The tobacco-specific nitrosamine 4-(methylnitrosamino)-1-(3-pyridyl)-1-butanone (NNK) is a potent lung carcinogen. Previously, we have demonstrated that NNK-induced lung tumorigenesis in mice depends on target-tissue bioactivation by pulmonary cytochrome P450 (P450) enzymes. The present study was designed to test the hypothesis that mouse CYP2A5 plays an essential role in NNK bioactivation in mouse lung. The role of CYP2A5 in NNK bioactivation was studied both in vitro and in vivo, by comparing kinetic parameters of microsomal NNK metabolism and tissue levels of O^6-mehtylguanine (O^6-mG) (the DNA adduct highly correlated with lung tumorigenesis) between wild-type (WT) and *Cyp2a5*-null mice. In both liver and lung microsomes, the loss of CYP2A5 resulted in significant increases in the apparent *Km* values for the formation of 4-oxo-4-(3-pyridyl)butanone (OPB), which represents the reactive intermediate that produces O^6-mG in vivo. The loss of CYP2A5 did not change circulating levels of NNK or 4-(methylnitrosamino)-1-(3-pyridyl)-1-butanol in mice treated intraperitoneally with NNK at either 20 or 100 mg/kg. However, the levels of lung O^6-mG were significantly lower in *Cyp2a5*-null than in WT mice; the extent of the reduction was greater at the 20 mg/kg dose (~40%) than at the 100 mg/kg dose (~20%). These results indicate that CYP2A5 is the low-*Km* enzyme for NNK bioactivation in mouse lung. Interestingly, the remaining NNK-bioactivation activities in the *Cyp2a5*-null mice could be inhibited by 8-methoxypsoralen, a P450 inhibitor utilized previously to demonstrate the role of CYP2A5 in NNK-induced lung tumorigenesis. Thus, P450 enzymes other than CYP2A5 probably also contribute to NNK-induced lung tumorigenesis in mice.

JPET Fast Forward. Published on January 19, 2012 as DOI: 10.1124/jpet.111.190173
This article has not been copyedited and formatted. The final version may differ from this version.

Introduction

The tobacco-specific nitrosamine 4-(methylnitrosamino)-1-(3-pyridyl)-1-butanone (NNK) is a potent lung procarcinogen in laboratory animals, and a human carcinogen (Hecht et al., 1989; IARC monograph 89, 2007). The carcinogenic effects of NNK depend on cytochrome P450 (P450)-mediated NNK α-hydroxylation at the methylene group or the methyl group, generating two distinct electrophilic intermediates, which can respectively methylate and pyridyloxobutylate DNA (Hecht, 1998). The methylene hydroxylation and methyl hydroxylation pathways also produce 4-oxo-4-(3-pyridyl)-butanone (OPB) and 4-hydroxy-1-(3-pyridyl)-1-butanone (HPB), respectively, which are used to represent activities of the respective α-hydroxylation pathways (Scheme 1). Multiple human and mouse P450s are active in the bioactivation of NNK *in vitro*, including human CYP1A, 2A, 2B, 2D, and 3A, and mouse CYP1A, 2A, and 2B enzymes (Smith et al., 1993; Hecht et al., 1998; Jalas et al., 2005). On the other hand, NNK can be metabolized by P450 to form NNK-N-oxide, which results in detoxification (Castonguay et al., 1983). NNK is also extensively reduced by carbonyl reductase in the liver, forming 4-(methylnitrosamino)-1-(3-pyridyl)-1-butanol (NNAL), the major circulating metabolite of NNK. Both NNAL and NNAL glucuronide are excreted in the urine (Hecht et al., 1998).

The formation and persistence of O^6-methylguanine (O^6-mG), through the methylene hydroxylation pathway, were found to be critical in the initiation of lung tumoregenesis by NNK in mice (Peterson et al., 1991a). The production of pyridyloxobutylated DNA, through the methyl hydroxylation pathway, also play an important role in NNK-induced lung tumorigenesis, as the pyridyloxobutyl DNA adducts can inhibit O^6-alkylguanine-DNA-alkyltransferase, the enzyme responsible for the repair of O^6-mG (Peterson et al., 1993). Gene mutations due to the formation of DNA adducts on the *K-ras* oncogene have been found to be characteristic of NNK-

JPET Fast Forward. Published on January 19, 2012 as DOI: 10.1124/jpet.111.190173
This article has not been copyedited and formatted. The final version may differ from this version.

induced lung tumors in mice (Ronai et al., 1993) and of smoking-related lung adenocarcinoma in humans (Ahrendt et al., 2001; Westra et al., 1993).

We have demonstrated previously that, while hepatic P450-mediated NNK metabolism influences the bioavailability of NNK in the lung, metabolic activation of NNK in the target tissue (the lung) plays an essential role in NNK-induced lung carcinogenesis (Weng et al., 2007). The specific P450 enzyme(s) responsible for NNK bioactivation in the lung have not been identified. Human CYP2A13, known to be expressed selectively in the respiratory tract (Su et al., 2000), displayed greater enzymatic efficiency in catalyzing both methyl and methylene α-hydroxylation of NNK than did any other P450 enzymes examined (Su et al., 2000; Jalas et al., 2005). It has been proposed that CYP2A13 plays a critical role in the bioactivation of NNK, and in NNK-induced initiation of lung cancer, in human smokers.

There is also evidence suggesting that CYP2A5, the ortholog of human CYP2A13 in mice, is essential for NNK bioactivation and tumorigenesis in the mouse lung. NNK readily induces lung adenocarcinoma following a single intraperitoneal injection of the carcinogen to mice (Hecht et al., 1989). CYP2A5, which is expressed in the lung, as well as in liver, kidney, and nasal mucosa (Su et al., 1996), is efficient in the bioactivation of NNK, as indicated by *in vitro* studies with recombinant CYP2A5 (Felicia et al., 2000; Jalas et al., 2003). Furthermore, NNK-induced lung tumorigenesis in mice was strongly inhibited by 8-methoxypsoralen (8-MOP) (Miyazaki et al., 2005), a compound often used as an inhibitor of CYP2A enzymes (Koenigs et al., 1997; von Weymarn et al., 2005; Visoni et al., 2005), although it is also capable of inhibiting CYP1A2 and CYP2E1 at higher concentrations (Labbe et al., 1987; Apseloff et al., 1991). However, direct proof for CYP2A5's or CYP2A13's role in mediating NNK bioactivation *in vivo* has yet to be obtained.

JPET Fast Forward. Published on January 19, 2012 as DOI: 10.1124/jpet.111.190173
This article has not been copyedited and formatted. The final version may differ from this version.

In the present study, we have directly determined the role of CYP2A5 in NNK bioactivation, both *in vitro* and *in vivo*, by comparing kinetic parameters of microsomal NNK metabolism and tissue levels of O^6-mG between wild-type (WT) and *Cyp2a5*-null mice. The *Cyp2a5*-null mouse model, produced through germline deletion of the last *Cyp2a5* coding exon, has been used successfully in studies on the role of CYP2A5 in the clearance of nicotine and cotinine (Zhou et al., 2010) and the bioactivation of nasal toxicants 2,6-dichlorobenzonitrile (Xie et al., 2010) and methimazole (Xie et al., 2011). Here, we present evidence that CYP2A5 is the low-*Km* enzyme for NNK bioactivation in mouse lung, and that P450s other than CYP2A5 probably also contribute to NNK-induced lung tumorigenesis in mice.

JPET Fast Forward. Published on January 19, 2012 as DOI: 10.1124/jpet.111.190173
This article has not been copyedited and formatted. The final version may differ from this version.

Methods

Chemicals and Reagents. HPB, (3,3,4,4-D_4)-4-hydroxy-1-(3-pyridyl)-1-butanone (D_4-HPB), NNK-N-oxide, and 4-oxo-4-(3-pyridyl)-butyric acid (OPBA) were purchased from Toronto Research Chemicals (Ontario, Canada); 8-MOP, sodium bisulfite, and reduced β-nicotinamide adenine dinucleotide phosphate (NADPH) were purchased from Sigma-Aldrich (St. Louis, MO). OPB was obtained from Santa Cruz Biotechnology (Santa Cruz, CA). The sources of NNK, NNAL, 4-(methylnitrosamino)-1-(3-[2,4,5,6-D_4]-pyridyl)-1-butanone (D_4-NNK), 4-(methylnitrosamino)-1-(3-[2,4,5,6-D_4]-pyridyl)-1-butanol (D_4-NNAL), O^6-mG, O^6-trideuteriomethyl-guanosine, O^6-methyl-deoxyguanosine and O^6-trideuteriomethyl-deoxyguanosine were the same as described previously (Weng et al., 2007). All solvents (acetonitrile, methanol, and water) were of high-performance liquid chromatography (LC) grade (ThermoFisher Scientific, Waltham, MA).

Determination of Catalytic Activity. Lung and liver microsomes were prepared as described (Ding and Coon, 1990). Protein concentration was determined by the bicinchoninic acid method (Pierce Chemical, Rockford, IL) with bovine serum albumin as the standard. For identification of microsomal NNK metabolites, assay mixtures contained 100 mM potassium phosphate buffer, pH 7.4, 10 μM NNK, 0.5 mg/ml liver or lung microsomal protein, 0 or 5 mM sodium bisulfite (as a trapping agent for OPB; Peterson et al., 1991b), and 1.0 mM NADPH, in a final volume of 0.2 ml. Reactions were carried out at 37°C for 30 min, and were terminated by the addition of 0.2 ml of acetonitrile. NADPH was omitted in negative control incubations. The apparent *Km* and *Vmax* values were determined using a broad range of NNK concentrations (0.5, 1, 2.5, 10, 25, 50, 100, 200 μM), with 0.25 mg/ml liver or lung microsomal protein from 2-month-old female WT A/J or B6 mice, or *Cyp2a5*-null mice (on B6 genetic background); the

JPET Fast Forward. Published on January 19, 2012 as DOI: 10.1124/jpet.111.190173
This article has not been copyedited and formatted. The final version may differ from this version.

reactions were carried out for 10 (for liver) or 30 (for lung) min, at 37°C, conditions under which the rates of product formation were linear with time, in the presence of 5 mM sodium bisulfite and 1 mM NADPH.

To determine the effects of 8-MOP on NNK bioactivation, 8-MOP (0, 0.5, or 2.5 μM) was first added (in 2 μl 50% methanol in H_2O) to "preincubation" mixtures consisting of 100 mM potassium phosphate buffer, pH 7.4, microsomal proteins (0.25 mg/ml) from 2-month-old *Cyp2a5*-null female mice, and 1 mM NADPH, in a total volume of 0.2 ml, and the mixture was incubated at 30°C for 20 min. NNK and sodium bisulfite were then added to the preincubation mixture, to final concentrations of 5 μM and 5 mM, respectively, and a final volume of 0.22 ml, and the incubation was continued at 30° C for another 10 (for liver) or 30 (for lung) min. A lower temperature (30^o C) was used, according to a published protocol (von Weymarn et al., 2005), in order to minimize NADPH-dependent activity losses in the control samples (with 0 μM 8-MOP).

For all reactions, internal standards (500 pg each of D_4-HPB and D_4-NNK) were added after the microsomal reactions were terminated with acetonitrile. The resultant mixtures were spun to remove precipitated protein; the supernatant was dried with nitrogen and then reconstituted in 50 μl of 50% (v/v) acetonitrile and 0.05% (w/v) formic acid in water for liquid chromatography-mass spectrometry (LC-MS) analysis.

Animal Studies. All procedures involving animals were approved by the Institutional Animal Care and Use Committee of the Wadsworth Center. For determination of NNK pharmacokinetics, 2-month-old WT B6 and *Cyp2a5*-null female mice were given a single intraperitoneal injection (at 9:00–10:00 A.M. local time) of NNK (at 20 or 100 mg/kg) in saline. Blood samples (~20 μl each) were collected from the tail of individual mice, at various time

JPET Fast Forward. Published on January 19, 2012 as DOI: 10.1124/jpet.111.190173
This article has not been copyedited and formatted. The final version may differ from this version.

points (10 min to 4 h) after the injection. The samples were centrifuged at 1000*g*, for 5 min, at 4°C, for preparation of plasma. For determination of tissue levels of O^6-mG DNA adduct, liver and lung were obtained at 4 h after NNK injection (at 20 or 100 mg/kg). For studies on in vivo inhibition of NNK clearance and bioactivation by 8-MOP, 2-month-old *Cyp2a5*-null female mice were pretreated via oral gavage with 8-MOP at 0 (vehicle control), 12.5, or 50 mg/kg in 0.2 ml corn oil, daily for 3 days, essentially as described previously (Takeuchi et al., 2003). One hour after the final dose of 8-MOP, NNK was given (at 100 mg/kg, i.p.) and the blood and tissue samples were collected as described above. Plasma and tissue samples were processed for LC-MS analysis of NNK/NNAL and O^6-mG, respectively, essentially as described earlier (Supplementary Materials in Weng et al., 2007).

LC-MS Analytical Methods. A LC-MS system composed of an Agilent 1200 Series high performance LC and an ABI 4000 Q-Trap mass spectrometer (Applied Biosystems, Foster City, CA) was used. Analytes were resolved using a 5-µm Gemini C18 column (100 x 2.0 mm, Phenomenex, Torrance, CA). The mass spectrometer was operated in a positive ion mode with an electrospay ionization source. The parameters for the chamber were as follows: curtain gas, 30 psi; heated nebulizer temperature, 350°C; ion spray voltage, 4500 V; nebulizer gas, 50 psi; turbo gas, 50 psi, declustering potential, 50 V; and entrance potential, 10 V.

For identification of NNK metabolites, the mobile phase consisted of solvent A (0.05% formic acid in water) and solvent B (0.05% formic acid in acetonitrile). Samples were eluted, at a flow rate of 0.3 ml/min, with 100% A for 2 min, followed by linear increases from 0% B to 100% B between 2 and 15 min, and then 100% B for a further 2.5 min. The mass spectrometer was set for the information-dependent acquisition scan mode, using multiple ion monitoring-dependent

enhanced product ion (MIM-EPI) acquisition, essentially as described by Yao and coworkers (Yao et al., 2008).

For quantitative analysis of NNK metabolites, shorter gradients (linear increase from 0% B to 90% B between 1 to 8 min, followed by a wash at 90% B for 2 min) were used, with formic acid either included (acidic condition, for OPB-bisulfite determination) or omitted (neutral condition, for HPB and NNK-N-oxide determination). Under acidic conditions, retention times for OPB-bisulfite, HPB (and D_4-HBP), NNK-N-oxide, and NNK (and D_4-NNK) were 5.5, 5.8, 6.2, and 6.7 min, respectively; under neutral condition, the retention times for HPB, NNK-N-oxide, and NNK were 6.5, 6.2, and 7.2 min, respectively, whereas OPB-bisulfite was unstable (as reported previously, Peterson et al., 1991b).

The parent/product ion pairs of *m/z* 166/106 (for HPB), *m/z* 224/177 (for NNK-N-oxide), *m/z* 246/164 (for bisulfite-trapped OPB), *m/z* 170/106 (for D_4-HPB), and *m/z* 212/126 (for D_4-NNK) (each representing transitions of the molecular ion to the most abundant product ion) were monitored in the multiple reaction monitoring (MRM) scan mode. For preparation of calibration curves, boiled microsomal preparations were mixed with increasing amounts of OPB, HPB, and NNK-N-oxide standards, in the presence of 5 mM sodium bisulfite. The standard mixtures were incubated, and then processed, as described above under *Determination of Catalytic Activity* for assay samples. The detection limits for OPB-bisulfite (246/164), HPB (166/106), and NNK-N-oxide (224/177) were 0.3, 0.03, and 0.05 pmol (on column), respectively. The recoveries for metabolite standards were > 80%.

The same LC-MS system was used for determination of the levels of NNK, NNAL, and O^6-mG, except that a shorter Gemini C18 column (5-µm, 50 x 2.0 mm, Phenomenex) was used, and the samples were eluted at a flow rate of 0.25 ml/min, with solvent A (water) and solvent B

(acetonitrile). The column was equilibrated with 100% A for 1 min, and the solvent gradient consisted of linear increases from 0% B to 100% B between 1 and 5 min, followed by a wash at 100% B for 2.5 min. The parent/product ion pairs of *m/z* 208/122 (for NNK), *m/z* 210/93 (for NNAL), *m/z* 212/126 (for D_4-NNK), *m/z* 214/97 (for D_4-NNAL), *m/z* 166/149 (for O^6-mG), and *m/z* 169/152 (for O^6-trideuteriomethyl-guanosine) were monitored in the MRM scan mode. The retention time was 6.1 min for O^6-mG and O^6-trideuteriomethyl-guanosine; 6.7 min for NNK and D_4-NNK; and 7.3 min for NNAL and D4-NNAL. Calibration curves for NNK, NNAL and O^6-mG were prepared, and levels of total guanine were determined, as described previously (Weng et al., 2007). The detection limits for NNK, NNAL, and O^6-mG were 0.05, 0.05, and 0.03 pmol (on column), respectively.

Statistics. Nonlinear regression and enzyme kinetic analyses were performed with use of GraphPad Prism 5 (GraphPad Software Inc., San Diego, CA). Student's *t* test was used for comparisons between two groups. One-way ANOVA (or one-way ANOVA on ranks when data failed normality test), followed by Tukey's post-hoc test (when p value is less than 0.05), was used for comparisons among multiple groups.

Results

Analysis of NNK Metabolite Formation Using LC-MS. Details of the LC-MS analysis for identification of NNK metabolites formed by mouse liver and lung microsomes (with or without the addition of sodium bisulfite for trapping the unstable OPB and preventing conversion of OPB to HPB) are shown in *Supplemental Material*, including total ion chromatograms of the MIM scans (Supplemental Fig. 1) and the MS/MS spectra obtained in the EPI scan mode for the detected metabolites (Supplemental Fig. 2). Identification of the parent compound (NNK *m/z*=208) and the stable metabolites (NNAL, *m/z*=212; HPB, *m/z*=166; OPBA, *m/z*=180; and NNK-N-oxide, *m/z*=224) was confirmed by co-elution with authentic standards and matching of MS/MS spectra. A standard for OPB-bisulfite was not available. The MS/MS spectrum of the assumed OPB-bisulfite molecular ion, at *m/z* 246, revealed two major product ions, at *m/z* 164 (loss of a sulfur dioxide and a water) and *m/z* 148 (loss of a sulfur trioxide and a water) (Supplemental Fig. 2E), both indicative of cleavage of the bisulfite moiety. The identification of OPB-bisulfite was further supported by the disappearance of OPBA (the oxidative product of OPB) upon inclusion of sodium bisulfite in the reaction mixture (Supplemental Fig. 1), and the bisulfite-dependent and OPB concentration-dependent formation of the *m/z* 246 ion in incubations of OPB with liver microsomes (data not shown).

Based on the qualitative data obtained in the MIM-EPI scan mode, methods for quantitative analysis of NNK-N-oxide, HPB, and OPB-bisulfite were established in the MRM scan mode. Typical LC-MS chromatograms for detection of the NNK metabolites are shown in Figure 1. It is notable that OPB-bisulfite, although barely detected in mouse lung microsomal incubations in the MIM-EPI scan mode (Supplemental Fig. 1), was readily detectable in the more sensitive MRM mode (Fig. 1). To test the validity of the LC-MS method, the apparent *Km* and

JPET Fast Forward. Published on January 19, 2012 as DOI: 10.1124/jpet.111.190173
This article has not been copyedited and formatted. The final version may differ from this version.

Vmax values for the formation of OPB and HPB by liver and lung microsomes from B6 and A/J female mice were determined (Supplemental Table 1); the kinetic parameters determined, which were nearly identical between A/J and B6 mice, were comparable to reported values (Peterson et al., 1991b; Nunes et al., 1998; Jalas et al., 2003).

Role of CYP2A5 in NNK Bioactivation in vitro. The contribution of CYP2A5 to NNK bioactivation in liver and lung microsomal reactions was determined by comparing activities between *Cyp2a5*-null mice (on B6 genetic background) and WT B6 mice. Female mice were studied, given the preferred use of female mice in NNK lung tumorigenesis bioassays (Hecht et al., 1989); *in vitro* NNK bioactivation by mouse lung and liver microsomes did not display obvious sex difference in the WT or *Cyp2a5*-null mice (data not shown). As shown in Table 1, the apparent *Km* values for the formation of OPB by lung microsomes from *Cyp2a5*-null mice were significantly higher than those of WT mice, although the *Vmax* values were not different. In contrast, there was no significant difference in the apparent *Km* and *Vmax* values for the formation of HPB, or the detoxification product, NNK-N-oxide. Higher *Km* and lower *Vmax* values were observed for the formation of HPB by liver microsomes from *Cyp2a5*-null mice than the values for WT B6 mice (Table 1). Higher *Km* values were also observed for the formation of OPB by liver microsomes from *Cyp2a5*-null mice, although the *Vmax* values remained unchanged. In contrast, no difference was observed in the kinetic parameters for the formation of NNK-N-oxide by liver microsomes from the WT and the *Cyp2a5*-null mice.

Pharmacokinetic Studies of Plasma NNK and NNAL in WT and *Cyp2a5*-null Mice. To determine whether the loss of CYP2A5 in the *Cyp2a5*-null mice impact systemic elimination of NNK and its major circulating metabolite NNAL, plasma levels of NNK and NNAL were measured in WT and *Cyp2a5*-null mice, following NNK administration at either 20 (Fig. 2A, B)

JPET Fast Forward. Published on January 19, 2012 as DOI: 10.1124/jpet.111.190173
This article has not been copyedited and formatted. The final version may differ from this version.

or 100 mg/kg (Fig. 2C, D). As expected, the pharmacokinetic profiles of plasma NNK or NNAL were not different between the two mouse strains, at either of the tested doses. The result indicated that neither hepatic, nor lung, CYP2A5 contributes significantly to the systemic clearance of NNK or NNAL.

Role of CYP2A5 in the Bioactivation of NNK in vivo. The levels of O^6-mG in the lung, which have been reported to correlate with incidences of lung tumors induced by NNK administration in mice (Peterson et al., 1991a), were determined as the genotoxic endpoint representing the extent of NNK's *in vivo* bioactivation, and its lung tumorigenic potential, in WT and *Cyp2a5*-null mice. The DNA adduct levels were determined at 4 h after NNK injection, a time point that was previously shown to display changes in adduct levels resulting from decreased NNK bioactivation in the lungs of the lung-*Cpr*-null mice (Weng et al., 2007). Following NNK treatment at 100 mg/kg, a standard dose used in lung tumorigenesis bioassays in mice (e.g., Weng et al., 2007), the levels of O^6-mG were found to be ~20% lower in the lungs of *Cyp2a5*-null than in the lungs of WT mice (Table 2). At a lower (20 mg/kg) NNK dose, the O^6-mG levels were >40% lower in the lungs of *Cyp2a5*-null than in the lungs of WT mice. These results indicate that CYP2A5 contributed to NNK bioactivation in the mouse lung *in vivo*, and that CYP2A5's contribution was much greater at the lower NNK dose tested, consistent with the results of in vitro studies showing that CYP2A5 is a low-*Km* enzyme for catalyzing the formation of OPB in lung microsomes (Table 1).

In contrast to the situation in the lung, the O^6-mG levels in the livers of WT and *Cyp2a5*-null mice were not different at 4 h after NNK treatment, at either dose. Thus, under the dosing conditions used, CYP2A5 does not contribute substantially to NNK bioactivation in the liver *in vivo*, despite the in vitro data showing that CYP2A5 is the low-*Km* enzyme for catalyzing the

formation of both OPB and HPB in liver microsomes (Table 1). This result is also consistent with the lack of an impact of the CYP2A5 loss on NNK systemic clearance in our pharmacokinetics study (Fig. 2).

Effects of 8-MOP on the Clearance and Bioactivation of NNK. The ability of orally administered 8-MOP (at 50 mg/kg or 12.5 mg/kg; Takeuchi et al., 2003) to inhibit NNK-induced lung tumorigenesis in female A/J mice was attributed to the inhibition by 8-MOP of CYP2A5-mediated NNK bioactivation (Miyazaki et al., 2005). Given our finding of a relatively high, remaining NNK bioactivation activity in the lungs of the *Cyp2a5*-null mice, we further tested whether the remaining bioactivation activities are also inhibited by 8-MOP, with NNK given at 100 mg/kg, as was in the original study (Takeuchi et al., 2003). Contrary to the lack of effects of CYP2A5 loss on NNK clearance (Fig. 2), the rates of NNK clearance were decreased in the *Cyp2a5*-null mice by pretreatment of mice with 8-MOP at 50 mg/kg, as indicated by the increased plasma NNK and NNAL levels at various time points after NNK administration (Fig. 3). However, despite the increased NNK bioavailability, the levels of O^6-mG in the lungs and livers were decreased, by ~70%, in the *Cyp2a5*-null mice pretreated with 8-MOP at 50 mg/kg (Table 3). In *Cyp2a5*-null mice pretreated with 8-MOP at the lower (12.5 mg/kg) dose, which did not result in a change in NNK clearance (Fig. 3), the levels of O^6-mG were also reduced, by 40% and 30%, in the livers and lungs, respectively (Table 3). These results, which indicate that the 8-MOP treatment in WT mice (Takeuchi et al., 2003; Miyazaki et al., 2005) inhibited not only CYP2A5, but also other P450s in the lungs and livers, strongly suggest that P450 enzymes other than CYP2A5 also contribute to NNK-induced lung tumorigenesis in the standard NNK lung tumor bioassay.

JPET Fast Forward. Published on January 19, 2012 as DOI: 10.1124/jpet.111.190173
This article has not been copyedited and formatted. The final version may differ from this version.

The effects of 8-MOP on NNK bioactivation were further investigated *in vitro*, using lung and liver microsomes from *Cyp2a5*-null mice, and using a 8-MOP preincubation scheme to mimic the pretreatment paradigm used *in vivo*, given the potential role of 8-MOP as mechanism-based, competitive, and non-competitive P450 inhibitors (Visoni et al., 2008). A pilot study (not shown) indicated that a 20-min preincubation with 8-MOP led to maximal inhibition of the activities toward NNK in either lung or liver microsomes from *Cyp2a5*-null mice. As shown in Figure 4, the formation of both OPB and HPB was inhibited, in a 8-MOP dose-dependent manner.

JPET Fast Forward. Published on January 19, 2012 as DOI: 10.1124/jpet.111.190173
This article has not been copyedited and formatted. The final version may differ from this version.

Discussion

The present study was designed to test the hypothesis that mouse CYP2A5 plays an essential role in NNK bioactivation in mouse lung, by comparing kinetic parameters of microsomal NNK metabolism and tissue levels of O^6-mG between WT and *Cyp2a5*-null mice. Recombinant CYP2A5 is very efficient in the bioactivation of NNK, producing both OPB and HPB (Felicia et al., 2000; Jalas et al., 2003). In the *Cyp2a5*-null mouse, the expression of CYP2A5, which is abundant in liver, lung and olfactory mucosa from WT mice, was abolished, and there was no compensatory change in the expression of other biotransformation enzymes examined, including multiple P450s and Phase II enzymes (Zhou et al., 2010; 2011). The suitability of the mouse model for studying the specific role of CYP2A5 in NNK bioactivation *in vivo* was further confirmed by the finding that the loss of CYP2A5 expression does not alter the rate of systemic clearance of NNK or its major circulating metabolite NNAL, a result indicating that the lungs of WT and *Cyp2a5*-null mice were exposed to similar levels of NNK and NNAL following the NNK treatment. Therefore, differences between the two mouse strains in the levels of lung DNA adducts detected were not because of differences in substrate (NNK) availability. In that connection, although CYP2A5 was abolished in all tissues of the *Cyp2a5*-null mice, the impact of the CYP2A5 loss on DNA adduct formation in the lung can be attributed to the contribution of lung CYP2A5, given our previous finding in a study on a lung-specific *Cpr*-null mouse that NNK-induced lung DNA adduct (O^6-mG) formation and tumorigenesis depends on target-tissue bioactivation by pulmonary P450 enzymes.

NNK metabolism was analyzed previously using radiometric LC assays, with use of [^{3}H]-NNK as the substrate (e.g., Zhang et al., 2007). An LC-MS protocol was developed here, in order to improve specificity and avoid the use of radioisotopes. The kinetic parameters were

JPET Fast Forward. Published on January 19, 2012 as DOI: 10.1124/jpet.111.190173
This article has not been copyedited and formatted. The final version may differ from this version.

nearly identical between A/J and B6 mice, for both liver and lung microsomal NNK metabolism, consistent with previous finding that the difference in sensitivity to NNK-induced lung tumorigenesis between A/J and B6 mice was not derived from a difference in NNK bioactivation (Devereux et al., 1993).

The contribution of CYP2A5 to the formation of O^6-mG *in vivo* was tissue- and NNK dose-dependent. The levels of lung O^6-mG were significantly lower in *Cyp2a5*-null than in WT mice; the extent of the reduction was greater at the 20 mg/kg dose (~40%) than at the 100 mg/kg dose (~20%). These results, which are consistent with *in vitro* data showing significant increases in the apparent *Km* values for the formation of OPB, the reactive intermediate that produces O^6-mG *in vivo*, in lung microsomes from *Cyp2a5*-null mice, indicate that CYP2A5 is the low-*Km* enzyme for NNK bioactivation in mouse lung. Intriguingly, although significant increases in the apparent *Km* values for the formation of OPB were also observed in liver microsomes from *Cyp2a5*-null mice, hepatic levels of O^6-mG in NNK-treated mice were not decreased or changed by the loss of CYP2A5 expression, at either of the NNK doses tested. A possible explanation for the apparent disparity between the *in vitro* and *in vivo* results is that, with NNK given via the intraperitoneal route in the *in vivo* experiments, the levels of NNK in the liver (the portal-of-entry organ), but not the lung, were much higher than the *Km* values of multiple hepatic P450s capable of bioactivating NNK, to the extent that a loss of the low-*Km* enzyme (CYP2A5) would not be noticed. On the other hand, the NNK concentrations tested *in vitro* included those similar to the *Km* values for CYP2A5, thus making it possible to reveal CYP2A5's activity in liver microsomes.

Our previous studies using a liver-specific *Cpr*-null mouse model showed that hepatic P450 enzymes are protective against NNK-induced lung tumorigenesis (Weng et al., 2007).

NNK can be detoxified via formation of NNK-N-oxide; although the specific mouse P450 enzymes responsible for NNK N-oxide formation have not been identified, rat CYP2B1 and CYP2C6 have been found to be active in NNK N-oxide formation (for a review see Jalas et al., 2005). Notably, our present data showed that the loss of CYP2A5 did not impact the rates of NNK-N-oxide formation in either liver or lung microcosms, indicating that CYP2A5 is not involved in this detoxification pathway.

The remaining activity of NNK bioactivation in the lung of *Cyp2a5*-null mice, which is rather high, may reflect the contributions by other P450 enzymes; members of several CYP subfamilies have been reported to be active in NNK bioactivation, including CYP1A, CYP2B, and CYP2F (Smith et al., 1993; Hecht et al., 1998). In addition, CYP2A4, although expressed in the lung at levels much lower than that of CYP2A5 (Su et al., 1996), displayed activity for NNK bioactivation (Jalas et al., 2005). In that connection, it is notable that, although CYP2A5 is a low-*Km* enzyme in the formation of HPB (Hecht et al., 1998), the contribution of CYP2A5 to the formation of HPB in mouse lung microsomes was negligible in our study. Thus, other low-*Km* enzymes, which are likely more abundant than CYP2A5 is in mouse lung microsomes, may play a more pivotal role in catalyzing the formation of HPB. Preliminary studies comparing lung microsomes from WT and *Cyp2f2*-null mice (Li et al., 2011) seem to indicate that mouse CYP2F2, which is highly abundant in lung microsomes, is another low-Km enzymes for the formation of HPB (Zhou et al., unpublished).

Our finding that remaining NNK-bioactivation activities in the *Cyp2a5*-null mice could be inhibited by 8-MOP, a P450 inhibitor utilized previously to demonstrate the role of CYP2A5 in NNK-induced lung tumorigenesis (Miyazaki et al., 2005), further supports the notion that P450 enzymes other than CYP2A5 also contribute to NNK-induced lung tumorigenesis in mice.

The ability of 8-MOP to act as a mechanism-based inhibitor of CYP2A enzymes has been well documented (Koenigs et al., 1997 and von Weymarn et al., 2005); 8-MOP was also found to inhibit mouse CYP2A5 through additional (competitive and non-competitive) mechanisms (Visoni et al., 2008). However, the specificity of inhibition of CYP2A enzymes by 8-MOP is not absolute, particularly at high 8-MOP concentration or doses; e.g., 8-MOP inhibited mouse hepatic microsomal metabolism of carbon tetrachloride, a CYP2E1 substrate, and caffeine, a CYP1A2 substrate, both *in vitro* and *in vivo* (Labbe et al., 1987; Apseloff et al., 1991).

Additional studies to directly demonstrate the role of CYP2A5, as well as other P450 enzymes, including CYP2F2 and CYP2B, in NNK-induced lung tumorigenesis are warranted. In that regard, the current *Cyp2a5*-null mouse is on the B6 genetic background, which is resistant to lung tumorigenesis. However, we have confirmed that there is no strain difference in NNK bioactivation in liver and lung microsomes between B6 and A/J mice; the latter is an established mouse strain for studies of NNK-induced lung tumorigenesis. Therefore, future studies for the role of CYP2A5 in NNK-induced lung tumorigenesis can be performed using *Cyp2a5*-null mice on the A/J background. In that connection, a recent study of a mouse model with targeted deletion of *Akt*, a putative oncogene closely linked to the *Cyp2a* locus on mouse chromosome 7, has already yielded indirect evidence that genetic variations in CYP2A5 can impact susceptibility to NNK-induced lung tumorigenesis in mice (Hollander et al., 2011).

Our demonstration of the role of CYP2A5 in NNK bioactivation in the mouse lung *in vivo* lends further support to the idea that human CYP2A13, which is even more efficient than mouse CYP2A5 is in NNK bioactivation (Jalas et al., 2005), is a susceptibility gene for NNK-induced lung carcinogenesis in humans. CYP2A13 protein is expressed in human lung (Zhu et al., 2006; Zhang et al., 2007). Levels of CYP2A13 protein expression correlated with rates of lung

microsomal NNK bioactivation (Zhang et al., 2007). Consistent with the evidence indicating that CYP2A13 is the most efficient enzyme for NNK bioactivation (Su et al., 2000; Jalas et al., 2005), a CYP2A13 genetic variation (*CYP2A13*2*), featuring a R257C change, which results in decreases both in CYP2A13 gene expression and in CYP2A13 metabolic activity toward NNK (Zhang et al., 2002; Schlicht et al., 2007; D'Agostino et al., 2008), has been associated with decreased incidences of lung adenocarcinoma in light smokers (Wang et al., 2003).

In conclusion, we proved that CYP2A5 is the low-*Km* enzyme for NNK bioactivation in the mouse lung, although P450 enzymes other than CYP2A5 also contribute. Our findings lay important foundation for further demonstration of the ability of human CYP2A13 to catalyze NNK bioactivation *in vivo* and to mediate NNK-induced lung tumorigenesis, through studies of a *CYP2A13*-transgenic mouse on a *Cyp2a5*-null genetic background.

Acknowledgements

We thank Ms. Yi Zhu for help with animal dosing, Ms. Weizhu Yang for technical assistance, and Dr. Qing-Yu Zhang for helpful discussions.

Authorship Contributions

Participated in research design: Zhou, D'Agostino, and Ding

Conducted experiments: Zhou, D'Agostino, Xie

Contributed new reagents or analytic tools: None

Performed data analysis: Zhou and Ding

Wrote or contributed to the writing of the manuscript: Zhou and Ding

Reference

Ahrendt SA, Decker PA, Alawi EA, Zhu Yr YR, Sanchez-Cespedes M, Yang SC, Haasler GB, Kajdacsy-Balla A, Demeure MJ, and Sidransky D (2001) Cigarette smoking is strongly associated with mutation of the K-ras gene in patients with primary adenocarcinoma of the lung. *Cancer* **92**:1525-1530.

Apseloff G, Hilliard JB, Gerber N, and Mays DC (1991) Inhibition and induction of drug metabolism by psoralens: alterations in duration of sleep induced by hexobarbital and in clearance of caffeine and hexobarbital in mice. *Xenobiotica* **21**:1461-1471.

Castonguay A, Stoner GD, Schut HA, and Hecht SS (1983) Metabolism of tobacco-specific N-nitrosamines by cultured human tissues. *Proc Natl Acad Sci U S A* **80**:6694-6697.

D'Agostino J, Zhang X, Wu H, Ling G, Wang S, Zhang QY, Liu F, and Ding X (2008) Characterization of CYP2A13*2, a variant cytochrome P450 allele previously found to be associated with decreased incidences of lung adenocarcinoma in smokers. *Drug Metab Dispos* **36**:2316-2323.

Devereux TR, Belinsky SA, Maronpot RR, White CM, Hegi ME, Patel AC, Foley JF, Greenwell A, and Anderson MW (1993) Comparison of pulmonary O6-methylguanine DNA adduct levels and Ki-ras activation in lung tumors from resistant and susceptible mouse strains. *Mol Carcinog* **8**:177-185.

Ding X, Coon MJ (1990) Immunochemical characterization of multiple forms of cytochrome P-450 in rabbit nasal microsomes and evidence for tissue-specific expression of P-450s NMa and NMb. *Mol Pharmacol* **37**:489-496.

Felicia ND, Rekha GK, and Murphy SE (2000) Characterization of cytochrome P450 2A4 and 2A5-catalyzed 4-(methylnitrosamino)-1-(3-pyridyl)-1-butanone (NNK) metabolism. *Arch Biochem Biophys* **384**:418-424.

Hecht SS, Morse MA, Amin S, Stoner GD, Jordan KG, Choi CI, and Chung FL (1989) Rapid single-dose model for lung tumor induction in A/J mice by 4-(methylnitrosamino)-1-(3-pyridyl)-1-butanone and the effect of diet. *Carcinogenesis* **10**:1901-1904.

Hecht SS (1998) Biochemistry, biology, and carcinogenicity of tobacco-specific N-nitrosamines. *Chem Res Toxicol* **11**:559-603.

IARC Monograph on the evaluation of carcinogenic risks to humans (2007). **89**: Smokeless tobacco and some tobacco-specific N-nitrosamine. Lyon, France: International Agency for Research on Cancer.

Jalas JR, Ding X, and Murphy SE (2003) Comparative metabolism of the tobacco-specific nitrosamines 4-(methylnitrosamino)-1-(3-pyridyl)-1-butanone and 4-(methylnitrosamino)-1-(3-pyridyl)-1-butanol by rat cytochrome P450 2A3 and human cytochrome P450 2A13. *Drug Metab Dispos* **31**:1199-1202.

Jalas JR, Hecht SS, and Murphy SE (2005) Cytochrome P450 enzymes as catalysts of metabolism of 4-(methylnitrosamino)-1-(3-pyridyl)-1-butanone, a tobacco specific carcinogen. *Chem Res Toxicol* **18**:95-110.

Koenigs LL, Peter RM, Thompson SJ, Rettie AE, and Trager WF (1997) Mechanism-based inactivation of human liver cytochrome P450 2A6 by 8-methoxypsoralen. *Drug Metab Dispos* **25**:1407-1415.

Labbe G, Descatoire V, Letteron P, Degott C, Tinel M, Larrey D, Carrion-Pavlov Y, Geneve J, Amouyal G, and Pessayre D (1987) The drug methoxsalen, a suicide substrate for cytochrome P-450, decreases the metabolic activation, and prevents the hepatotoxicity, of carbon tetrachloride in mice. *Biochem Pharmacol* **36**:907-914.

Li L, Wei Y, Van Winkle L, Zhang QY, Zhou X, Hu J, Xie F, Kluetzman K, Ding X (2011) Generation and characterization of a *Cyp2f2*-null mouse and studies on the role of CYP2F2 in naphthalene-induced toxicity in the lung and nasal olfactory mucosa. *J Pharmacol Exp Ther* in press.

Miyazaki M, Yamazaki H, Takeuchi H, Saoo K, Yokohira M, Masumura K, Nohmi T, Funae Y, Imaida K, and Kamataki T (2005) Mechanisms of chemopreventive effects of 8-methoxypsoralen against 4-(methylnitrosamino)-1-(3-pyridyl)-1-butanone-induced mouse lung adenomas. *Carcinogenesis* **26**:1947-1955.

Nunes MG, Desai D, Koehl W, Spratt TE, Guengerich FP, and Amin S (1998) Inhibition of 4-(methylnitrosamino)-1-(3-pyridyl)-1-butanone (NNK) metabolism in human hepatic microsomes by ipomeanol analogs--an exploratory study. *Cancer Lett* **129**:131-138.

Peterson LA and Hecht SS (1991a) O6-methylguanine is a critical determinant of 4-(methylnitrosamino)-1-(3-pyridyl)-1-butanone tumorigenesis in A/J mouse lung. *Cancer Res* **51**:5557-5564.

Peterson LA, Mathew R, and Hecht SS (1991b) Quantitation of microsomal alpha-hydroxylation of the tobacco-specific nitrosamine, 4-(methylnitrosamino)-1-(3-pyridyl)-1-butanone. *Cancer Res* **51**:5495-5500.

Peterson LA, Liu XK, and Hecht SS (1993) Pyridyloxobutyl DNA adducts inhibit the repair of O6-methylguanine. *Cancer Res* **53**:2780-2785.

Ronai ZA, Gradia S, Peterson LA, and Hecht SS (1993) G to A transitions and G to T transversions in codon 12 of the Ki-ras oncogene isolated from mouse lung tumors induced by 4-(methylnitrosamino)-1-(3-pyridyl)-1-butanone (NNK) and related DNA methylating and pyridyloxobutylating agents. *Carcinogenesis* **14**:2419-2422.

Schlicht KE, Michno N, Smith BD, Scott EE, and Murphy SE (2007) Functional characterization of CYP2A13 polymorphisms. *Xenobiotica* **37**:1439-1449.

Smith TJ, Guo Z, Li C, Ning SM, Thomas PE, and Yang CS (1993) Mechanisms of inhibition of 4-(methylnitrosamino)-1-(3-pyridyl)-1-butanone bioactivation in mouse by dietary phenethyl isothiocyanate. *Cancer Res* **53**, 3276-3282.

Su T, Sheng JJ, Lipinskas TW, and Ding X (1996) Expression of CYP2A genes in rodent and human nasal mucosa. *Drug Metab Dispos* **24**:884-890.

Su T, Bao Z, Zhang QY, Smith TJ, Hong JY, and Ding X (2000) Human cytochrome P450 CYP2A13: predominant expression in the respiratory tract and its high efficiency metabolic activation of a tobacco-specific carcinogen, 4-(methylnitrosamino)-1-(3-pyridyl)-1-butanone. *Cancer Res* **60**:5074-5079.

Takeuchi H, Saoo K, Yokohira M, Ikeda M, Maeta H, Miyazaki M, Yamazaki H, Kamataki T, and Imaida K (2003) Pretreatment with 8-methoxypsoralen, a potent human CYP2A6 inhibitor, strongly inhibits lung tumorigenesis induced by 4-(methylnitrosamino)-1-(3-pyridyl)-1-butanone in female A/J mice. *Cancer Res* **63**:7581-7583.

Visoni S, Meireles N, Monteiro L, Rossini A, and Pinto LF (2008) Different modes of inhibition of mouse Cyp2a5 and rat CYP2A3 by the food-derived 8-methoxypsoralen. *Food Chem Toxicol* **46**:1190-1195.

von Weymarn LB, Zhang QY, Ding X, and Hollenberg PF (2005) Effects of 8-methoxypsoralen on cytochrome P450 2A13. *Carcinogenesis* **26**:621-629.

Wang H, Tan W, Hao B, Miao X, Zhou G, He F, and Lin D (2003) Substantial reduction in risk of lung adenocarcinoma associated with genetic polymorphism in CYP2A13, the most active cytochrome P450 for the metabolic activation of tobacco-specific carcinogen NNK. *Cancer Res* **63**:8057-8061.

Weng Y, Fang C, Turesky RJ, Behr M, Kaminsky LS, and Ding X (2007) Determination of the role of target tissue metabolism in lung carcinogenesis using conditional cytochrome P450 reductase-null mice. *Cancer Res* **67**:7825-7832.

Westra WH, Slebos RJ, Offerhaus GJ, Goodman SN, Evers SG, Kensler TW, Askin FB, Rodenhuis S, and Hruban RH (1993) K-ras oncogene activation in lung adenocarcinomas from former smokers. Evidence that K-ras mutations are an early and irreversible event in the development of adenocarcinoma of the lung. *Cancer* **72**:432-438.

Xie F, Zhou X, Behr M, Fang C, Horii Y, Gu J, Kannan K, Ding X (2010) Mechanisms of olfactory toxicity of the herbicide 2,6-dichlorobenzonitrile: essential roles of CYP2A5 and target-tissue metabolic activation. *Toxicol Appl Pharmacol.* **249**: 101-106.

Xie F, Zhou X, Genter MB, Behr M, Gu J, Ding X (2011) The tissue-specific toxicity of methimazole in the mouse olfactory mucosa is partly mediated through target-tissue metabolic activation by CYP2A5. *Drug Metab Dispos.* **39**:947-951.

Yao M, Ma L, Humphreys WG, and Zhu M (2008) Rapid screening and characterization of drug metabolites using a multiple ion monitoring-dependent MS/MS acquisition method on a hybrid triple quadrupole-linear ion trap mass spectrometer. *J Mass Spectrom* **43**:1364-1375.

Zhang X, Su T, Zhang QY, Gu J, Caggana M, Li H, and Ding X (2002) Genetic polymorphisms of the human CYP2A13 gene: identification of single-nucleotide polymorphisms and functional characterization of an Arg257Cys variant. *J Pharmacol Exp Ther* **302**:416-423.

Zhang X, D'Agostino J, Wu H, Zhang QY, von Weymarn L, Murphy SE, and Ding X (2007) CYP2A13: variable expression and role in human lung microsomal metabolic activation of the tobacco-specific carcinogen 4-(methylnitrosamino)-1-(3-pyridyl)-1-butanone. *J Pharmacol Exp Ther* **323**:570-578.

Zhou X, Zhuo X, Xie F, Kluetzman K, Shu YZ, Humphreys WG, and Ding X (2010) Role of CYP2A5 in the clearance of nicotine and cotinine: insights from studies on a *Cyp2a5*-null mouse model. *J Pharmacol Exp Ther* **332**:578-587.

Zhou X, Wei Y, Xie F, Laukaitis C, Karn R, Kluetzman K, Gun J, Zhang Q-Y, Roberts D and Ding X (2011) A novel defensive mechanism against acetaminophen toxicity in the mouse lateral nasal gland: role of CYP2A5-mediated regulation of testosterone

homeostasis and salivary androgen-binding protein expression. *Mol Pharmacol* **79**:710-723.

Zhu LR, Thomas PE, Lu G, Reuhl KR, Yang GY, Wang LD, Wang SL, Yang CS, He XY, and Hong JY (2006) CYP2A13 in human respiratory tissues and lung cancers: an immunohistochemical study with a new peptide-specific antibody. *Drug Metab Dispos* **34**:1672-1676.

Footnotes

This work was supported in part by the National Institutes of Health National Cancer Institute [Grant CA092596].

Address correspondence to: Dr. Xinxin Ding, Wadsworth Center, New York State Department of Health, Empire State Plaza, Box 509, Albany, NY 12201-0509. E-mail: xding@wadsworth.org

Figure Legends

Scheme 1. P450-mediated biotransformation of NNK (Modified from Jalas et al., 2005).

Fig. 1. Typical LC-MS chromatograms for detection of NNK metabolites. Extracted LC-MS chromatograms, for individual metabolites detected in reactions with liver (A-C) and lung (D-F) microsomes from WT mice, obtained in the MRM scan mode for quantitative analysis of metabolite levels, are shown for HPB (A, D), NNK-N-oxide (B, E), and OPB-bisulfite (C, F), with NNK substrate concentration at 2.5 μM. The chromatograms for OPB-bisulfite were obtained under acidic condition, whereas those for HPB and NNK-N-oxide were obtained under neutral condition. Microsomal incubations were performed without (negative controls) or with NADPH, and sodium bisulfite was added to some samples to trap OPB, as described in *Methods*. No signal was detected when NADPH was omitted from the incubations (data not shown). The parent/product ion pairs of m/z 166/106 (for HPB), m/z 224/177 (for NNK-N-oxide), m/z 246/164 (for bisulfite-trapped OPB) were monitored. Metabolite identification using the MIM-EPI acquisition mode and the resultant MS/MSproduct-ion spectra of the detected metabolites are shown in Supplemental Figures 1 and 2.

Fig. 2. Comparisons of NNK and NNAL clearance between WT and *Cyp2a5*-null mice. WT B6 and *Cyp2a5*-null mice (2-month-old, female) were injected with NNK 20 (A, B) or 100 mg/kg (C, D) i.p., and levels of NNK (A, C) and NNAL (B, D) were determined in the plasma, at various times after the injection. Data represent means ± S.D. (n = 4). No significant difference was found between the two strains, at any time point, for either NNK or NNAL (Student's t-test).

Fig. 3. Effects of 8-MOP pretreatment on the clearance of NNK and NNAL in the *Cyp2a5*-null mice. Mice (2- to 3-month old, female) were pretreated with 8-MOP (at 0, 12.5, or 50 mg/kg, in 0.2 ml corn oil, via oral gavage) once daily for 3 consecutive days. NNK was administered (at 100 mg/kg, i.p.) at 1 h after the final dose of 8-MOP. Data represent means ± S.D., n = 4. **, $p <$ 0.01, *, $p < 0.05$, compared to the 0-mg/kg 8-MOP (vehicle alone) group (One-way ANOVA, followed by Tukey's post-hoc test)

Fig. 4. The effects of 8-MOP on NNK bioactivation in lung and liver microsomes from *Cyp2a5*-null mice. The rates of formation of OPB and HPB were determined for lung (top) and liver (bottom) microsomal samples that had been pre-incubated with 0, 0.5, or 2.5 μM 8-MOP, as described in *Methods*, with NNK at 5 μM. Values represent means ± S.D. of data from three separate microsomal samples, each prepared from pooled tissues from five 2-month-old female *Cyp2a5*-null mice. **, $p < 0.01$, compared with the 0-μM 8-MOP group (One-way ANOVA followed by Tukey's post-hoc test). The extents of inhibition (%) are indicated.

JPET Fast Forward. Published on January 19, 2012 as DOI: 10.1124/jpet.111.190173
This article has not been copyedited and formatted. The final version may differ from this version.

TABLE 1

Kinetic parameters for the formation of NNK metabolites by mouse lung and liver microsomes

Apparent Km and Vmax values for the microsomal formation of three major NNK metabolites (HPB, NNK-N-oxide, and sodium bisulfite-trapped OPB) were determined as described in *Methods*. Values represent means ± S.D. of values determined for three separate microsomal samples, each prepared from tissues pooled from five 2-month-old female mice.

Metabolite	Strain	Lung			Liver		
		Km (μM)	*Vmax* (*pmol/min/mg*)	*Vmax/Km*	*Km (μM)*	*Vmax* (*pmol/min/mg*)	*Vmax/Km*
OPB	WT (B6)	28.0 ± 1.9	57.3 ± 1.8	2.0	29 ± 4	220 ± 10	7.6
	Cyp2a5-null	40.2 ± 2.1[a]	61.5 ± 2.0	1.5	55 ± 5[a]	210 ± 10	4.0
HPB	WT (B6)	2.8 ± 0.3	24.3 ± 0.5	8.7	18 ± 3	105 ± 5	5.9
	Cyp2a5-null	2.9 ± 0.3	24.4 ± 1.0	8.4	65 ± 15[a]	70 ± 8[a]	1.1
NNK-N-oxide	WT (B6)	1.6 ± 0.2	35.8 ± 3.1	22.4	84 ± 18	19 ± 2	0.2
	Cyp2a5-null	1.9 ± 0.3	38.7 ± 2.2	20.4	83 ± 16	20 ± 2	0.2

[a] $p < 0.01$, compared with WT mice, Student's t-test

TABLE 2

NNK-induced O^6-mG adduct formation in the liver and lung

Two-month-old, WT B6 and *Cyp2a5*-null female mice were injected with NNK at a dose of 20 or 100 mg/kg (i.p.), and tissue levels of O^6-mG and total guanine were determined at 4 h after the injection, as described in *Methods*. Data represent means ± S.D. (n = 8).

NNK Dose (*mg/kg*)	Strain	O^6-mG Level (*pmol/µmol guanine*)	
		Lung	Liver
20	WT (B6)	5.4 ± 0.5	115 ± 13
	Cyp2a5-null	3.3 ± 0.8[a]	108 ± 18
100	WT (B6)	23.6 ± 1.6	594 ± 70
	Cyp2a5-null	18.8 ± 1.7[b]	604 ± 48

[a] $p < 0.01$; [b] $p < 0.05$; compared with WT mice; Student's t-test

TABLE 3

Effects of 8-MOP on NNK-induced O^6-mG adduct formation in the liver and lung of *Cyp2a5*-null mice

Two-month-old, female *Cyp2a5*-null mice were pretreated with 8-MOP (at 0, 12.5, or 50 mg/kg, p.o.) in 0.2 ml corn oil, once daily for three consecutive days. One hour after the final injection of 8-MOP, NNK was given at a dose of 100 mg/kg (i.p.), and tissue levels of O^6-mG and total guanine were determined at 4 h after the NNK injection. Data represent means ± S.D. (n = 4).

8-MOP Dose (*mg/kg*)	O^6-mG Level (*pmol/µmol guanine*)	
	Lung	Liver
0	19.0 ± 1.8	590 ± 21
12.5	13.4 ± 1.5[b]	337 ± 70[a]
50	6.2 ± 3.0[a]	170 ± 99[a]

[a] $p < 0.01$, [b] $p<0.05$, compared with the 0 mg/kg 8-MOP (vehicle control) group (One-way ANOVA followed by Tukey's post-hoc test)

JPET Fast Forward. Published on January 19, 2012 as DOI: 10.1124/jpet.111.190173
This article has not been copyedited and formatted. The final version may differ from this version.

Scheme 1

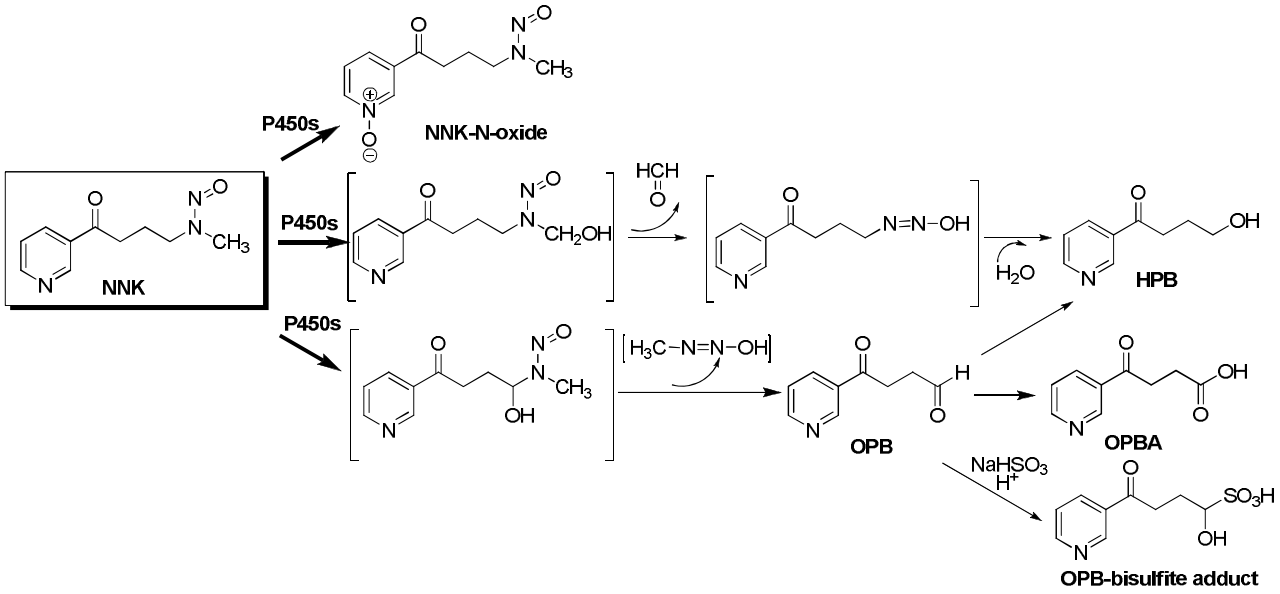

JPET Fast Forward. Published on January 19, 2012 as DOI: 10.1124/jpet.111.190173
This article has not been copyedited and formatted. The final version may differ from this version.

Fig. 1

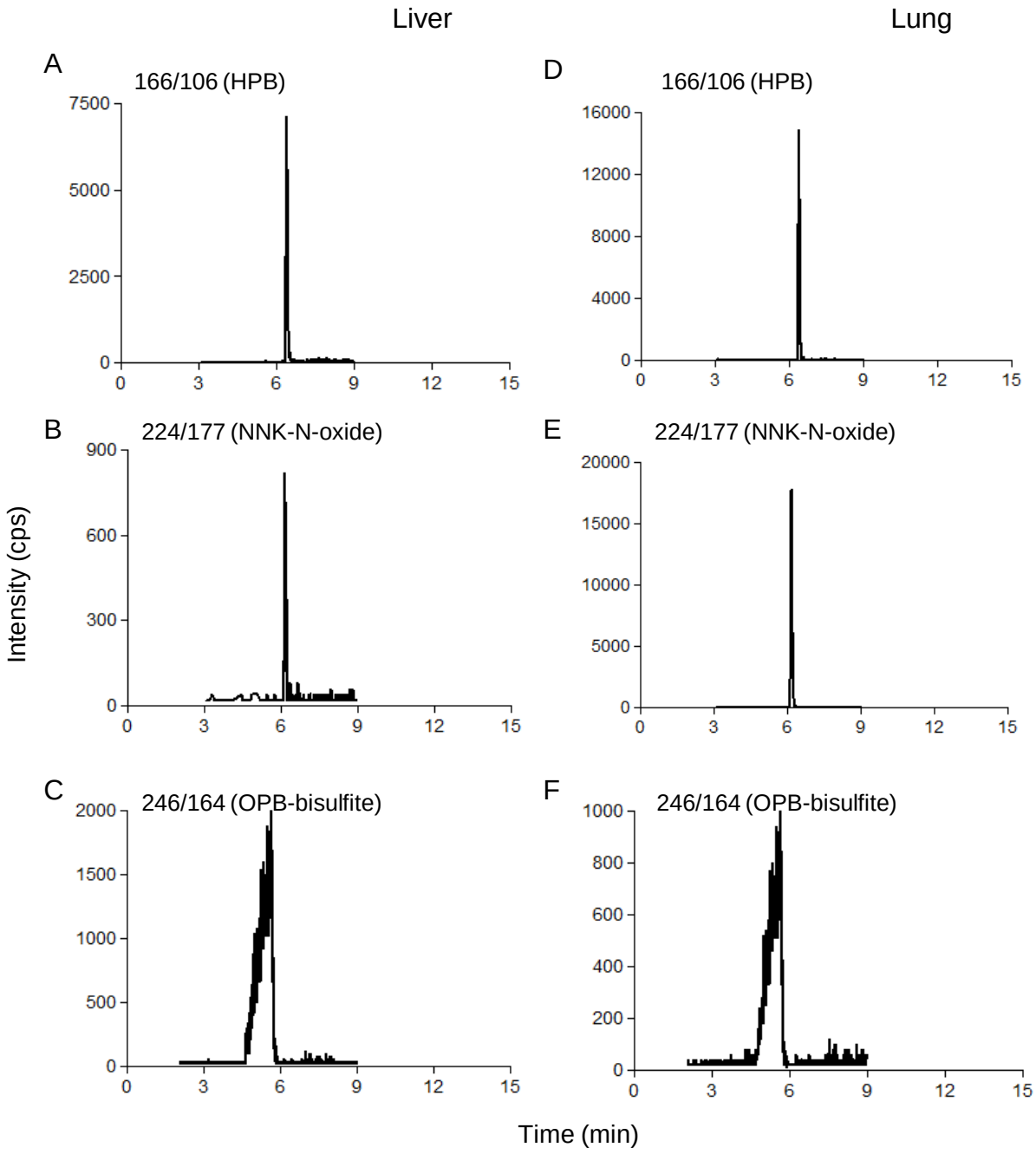

JPET Fast Forward. Published on January 19, 2012 as DOI: 10.1124/jpet.111.190173
This article has not been copyedited and formatted. The final version may differ from this version.

Fig. 2

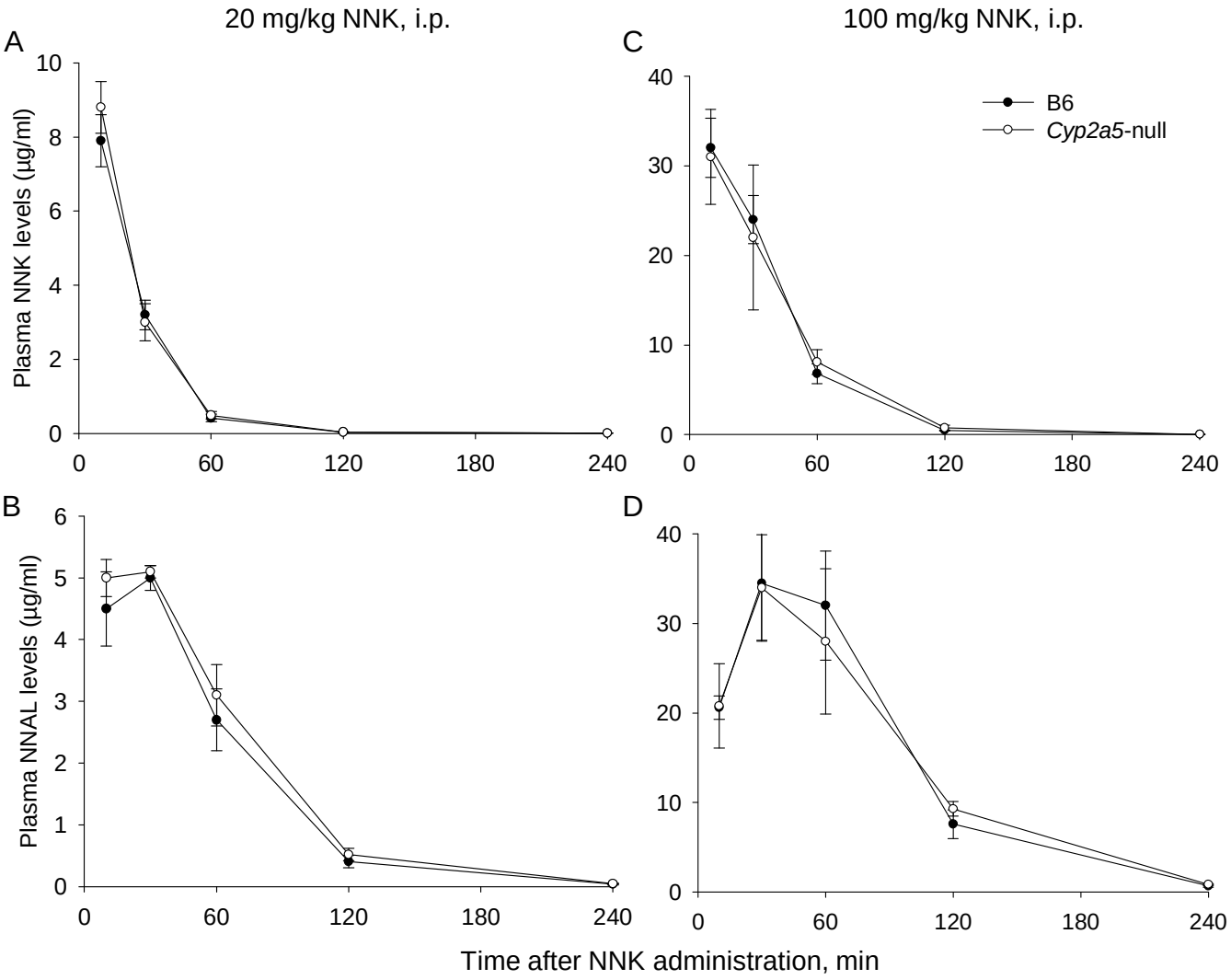

JPET Fast Forward. Published on January 19, 2012 as DOI: 10.1124/jpet.111.190173
This article has not been copyedited and formatted. The final version may differ from this version.

Fig. 3

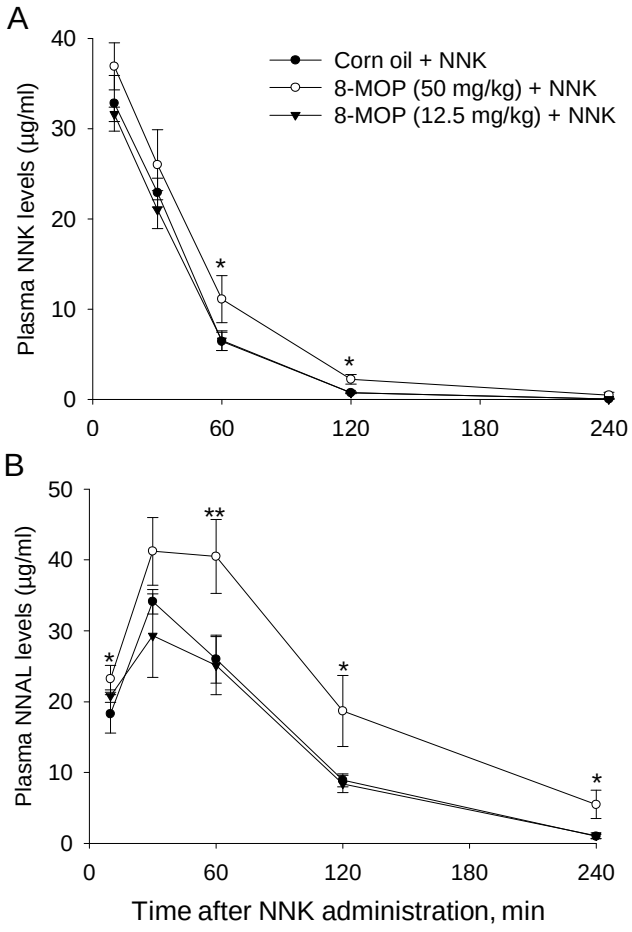

JPET Fast Forward. Published on January 19, 2012 as DOI: 10.1124/jpet.111.190173
This article has not been copyedited and formatted. The final version may differ from this version.

Fig. 4